

Article

# Proton- and Neutron-Induced SEU Cross-Section Modeling and Simulation: A Unified Analytical Approach

Gennady I. Zebrev<sup>1</sup>, Nikolay N. Samotaev<sup>1,\*</sup>, Rustem G. Useinov<sup>2</sup>, Artur M. Galimov<sup>3</sup>, Vladimir V. Emeliyanov<sup>2</sup>, Artyom A. Sharapov<sup>2</sup>, Dmitri A. Kazyakin<sup>1,3</sup> and Alexander S. Rodin<sup>1</sup>

<sup>1</sup> Micro- and Nanoelectronics Department, National Research Nuclear University MEPhI (Moscow Engineering Physics Institute), 115409 Moscow, Russia

<sup>2</sup> Research Institute of Scientific Instruments, Lytkarino, 140061 Moscow, Russia; vemeliyanov@niipribor.ru (V.V.E.); s.artem11@mail.ru (A.A.S.)

<sup>3</sup> MRI Progress, 109028 Moscow, Russia

\* Correspondence: nnsamotaev@mephi.ru

**Simple Summary:** Disturbances (so called single event upsets) in the operation of digital electronics due to primary ionizing particles as well as to secondary products of nuclear reactions is a fundamental problem for space and industrial systems. The processes involved are very complex, and the existing cumbersome software packages for circuits and nuclear interaction simulations are conceptually poorly compatible and not themselves designed to describe this type of upsets. For prediction purposes, we have proposed a simple but rather general analytical computational scheme within which the nuclear and circuit parts of the modeling can be consistently combined. The proposed analytical approach uses only physics-based or circuit parameters that can be measured or refined by simulations with standard software packages. Using this approach significantly simplifies and speeds up the design of reliability of digital computing systems in hostile environments.

**Abstract:** A new physics-based compact model, which makes it possible to simulate in a unified way the neutrons and protons of cosmic ray-induced SEU cross-sections, including the effects from nuclear reaction products and from direct ionization by low-energy protons, has been proposed and validated. The proposed approach is analytical and based on explicit analytical relationships and approximations with physics-based fitting parameters. GEANT4 or SRIM numerical calculations can be used as an aid to adjust or refine the phenomenological parameters or functions included in the model, taking into account real geometrical configurations and chemical compositions of the devices. In particular, explicit energy dependencies of the soft error cross-sections for protons and neutrons over a wide range of nucleon energies were obtained and validated. The main application areas of the developed model include space physics, accelerator studies high energy physics and nuclear experiments.

**Keywords:** direct ionization; low-energy protons; modeling; neutrons; nuclear reactions; SEU cross-sections; single-event upsets



**Citation:** Zebrev, G.I.; Samotaev, N.N.; Useinov, R.G.; Galimov, A.M.; Emeliyanov, V.V.; Sharapov, A.A.; Kazyakin, D.A.; Rodin, A.S. Proton- and Neutron-Induced SEU Cross-Section Modeling and Simulation: A Unified Analytical Approach. *Radiation* **2024**, *4*, 37–49. <https://doi.org/10.3390/radiation4010004>

Academic Editor: Ehsan Nazemi

Received: 26 December 2023

Revised: 29 January 2024

Accepted: 10 February 2024

Published: 14 February 2024



**Copyright:** © 2024 by the authors. Licensee MDPI, Basel, Switzerland. This article is an open access article distributed under the terms and conditions of the Creative Commons Attribution (CC BY) license (<https://creativecommons.org/licenses/by/4.0/>).

## 1. Introduction

Soft errors (or single-event upsets, SEUs), i.e., the reversible changes in digital devices' states caused by one single ionizing particle, are one of the main challenges of modern digital electronics [1]. The main sources of such errors in space satellites and in avionics are the nuclear interactions of protons and neutrons with atoms of the material of electronic circuits. The soft error rate (SER) or cross-section prediction of nucleon-induced SEU faces great difficulties because the circuit and the nuclear interaction simulators are poorly compatible technically and conceptually. Furthermore, aggressive scaling of the microelectronics components leads to decreased immunity of the digital integrated circuits

to external transients due to the reduction in the noise margin due to the lowering of the supply voltage and the reduction in the element size. In particular, the commercial highly-scaled digital memories become extremely susceptible to the single-event effects (SEE). For example, the critical charge  $Q_C$ , i.e., the minimum charge to cause an upset of the memory cell, reduces to the sub-femtocoulomb region. Such values of the collected charge (of order  $10^3$ – $10^4$  carriers) correspond to the mean deposited energy as small as a few keV and average values of critical linear energy transfer (LET) less than 1 MeV-cm<sup>2</sup>/mg. For example, the circuit critical charge  $\varepsilon_C$  can be mapped to the transferred critical energy required to switch the digital element [2].

$$\varepsilon_C = \frac{Q_C}{q} \varepsilon_p = 22.5 \left( \frac{Q_C}{fC} \right) \text{ keV}, \quad (1)$$

where  $\varepsilon_p \cong 3.6$  eV(Si) is the mean energy of electron–hole creation [2]. It is important to emphasize that  $\varepsilon_C$  and  $Q_C$  are, as a rule, the purely circuit parameters that characterize the immunity of a typical digital node to transient electrical disturbances of any origin. The probability (cross-section) of a nucleon-induced error becomes noticeable when the local energy release from the products of a nuclear reaction and linear energy transfer (LET) of nuclear reaction products exceed a critical value  $\Lambda_{\text{sec}} > \Lambda_C \propto \varepsilon_C$ , where  $\Lambda_{\text{sec}}$  is a typical LET of secondary particles. Since the LET of direct ionization from protons is small, it has long been reasonably assumed that when exposed to protons, a necessary condition for soft error generation is a proton-induced nuclear reaction. Nevertheless, the technologically driven decrease in  $\varepsilon_C$  and  $Q_C$  leads to the fact that single-event upsets in digital circuits can be caused by direct ionization of particles even with a very small LET value, such as by low-energy protons [3–5].

Another challenge is the neutron-induced soft error rate (SER), arising from the finite value of the neutron flux in the atmosphere or even at the sea level ( $\sim 13 \text{ cm}^{-2} \text{ h}^{-1}$ ) [6–9]. The physical processes involved in the failure mechanisms from neutrons and low-energy protons are quite complex and strictly speaking require cumbersome computational approaches based on numerical simulations (e.g., GEANT4, TCAD or MRED) [10–12]. Such systems are often inaccessible, inconvenient to use and require highly skilled users.

In this study, we propose a variant of a compact model for the calculation of the SEU cross-sections induced by protons, neutrons and direct ionization (including by low-energy protons) based on transparent physical models and controlled approximations. We will demonstrate here that even such seemingly heterogeneous problems, such as modeling of the SEU cross-sections caused by secondary products of nuclear reactions and by low-energy proton direct ionization, can be readily simulated within the framework of a unified approach. The main motivation of this study is to try to replace the cumbersome and opaque GEANT4 numerical simulation with a simple and transparent analytical model with physically measured and calculated parameters.

## 2. Methodology

### 2.1. A General Framework

The suggested model is intended to first analyze the SEU rate in regularly arranged electronic devices such as memory circuits. There are two types of the single-event errors, namely the errors due to direct ionization of primary particles and errors due to ionization by the secondary products of elastic or non-elastic nuclear interactions formed upon irradiation with the primary particles. Both types are determined ultimately by direct ionization with heavy ions of either primary or secondary origin. The volume in which charge separation and collection occurs is commonly referred to as the sensitive volume [13]. Due to the nonlocality of the ion impact, the concept of a sensitive volume for an individual memory cell is violated, since the entire memory area is a single sensitive volume with an effective thickness  $t_{\text{eff}}$  [14]. This effective thickness turns out to be quite small ( $\geq 10$  nm) for ICs with sub-femtocoulomb  $Q_C$ . At the same time, the thickness of the region in which nuclear reactions occur, affecting the ionization in the sensitive region, is of the order of the

secondary particle range ( $L_R \geq 1 \mu\text{m}$ ). Conceptually, these are two completely different regions, one of which is determined by circuit factors (simulated with CAD or TCAD) and the other by nuclear physics (GEANT4). The region of actual nuclear reactions will be referred to below as the influencing region (see Figure 1).

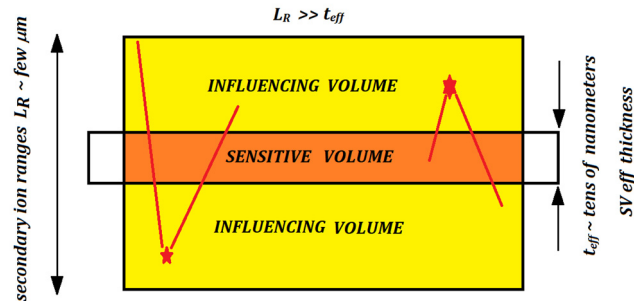


**Figure 1.** Conceptual view of influencing and sensitive volumes.

The influencing volume, where actual nuclear reactions take place, is typically much larger than the sensitive volume where the charge is collected ( $L_R \gg t_{eff}$ ). This allows us to represent the sensitive region as being affected by a flow of secondary ions with its own differential LET spectrum  $\Phi_{sec}(\Lambda)$  (here,  $\Lambda$  is LET, for brevity). Then, the expected value of the error number per memory cell with a fixed critical charge  $Q_C$  (or, similarly, the soft error rate per bit (SER)) can be generally calculated as follows [15]:

$$N(Q_C) = \int \sigma(\Lambda|Q_C) \Phi_{sec}(\Lambda) d\Lambda, \quad (2)$$

where  $\sigma(\Lambda|Q_C)$  is the LET-dependent direct ionization-induced cross-sections for secondary particles and  $\Phi_{sec}(\Lambda)$  is a differential LET spectrum of secondary particles for a given period of time. The spectrum  $\Phi_{sec}(\Lambda)$  depends on the cross-sections of the nuclear interactions, and also on the integrated circuit characteristics (layout, chemical composition, overlayer structure, etc.) within the influencing volume with spatial scales  $\sim L_R$  significantly exceeding the charge collection length.

The same value can be calculated as a result of the impact of primary nucleons (neutrons or protons) using the nucleon cross-section concept  $\sigma_n(\varepsilon_n|Q_C)$ :

$$N(Q_C) = \int \sigma_n(\varepsilon_n|Q_C) \Phi_n(\varepsilon_n) d\varepsilon_n, \quad (3)$$

where  $\Phi_n(\varepsilon_n)$  is the primary nucleon energy spectrum. The energy of each primary nucleon corresponds to its own LET spectrum of secondary particles, which can be approximated somehow or simulated with GEANT4. The LET spectrum of secondary particles from nucleons of all energies can be written in this form:

$$\Phi_{sec}(\Lambda) = \int \alpha(\Lambda|\varepsilon_n) \Phi(\varepsilon_n) d\varepsilon_n, \quad (4)$$

where a conversion function  $\alpha(\Lambda|\varepsilon_n)$  transforms an energy spectrum of primary particles to a LET spectrum of secondary particles.

Equations (2) and (3) are fully consistent and equivalent under the linear integral relation:

$$\sigma_n(\varepsilon_n|Q_C) = \int \alpha(\Lambda|\varepsilon_n) \sigma(\Lambda|Q_C) d\Lambda. \quad (5)$$

This can be verified directly by substituting (5) into (3) and changing the order of the integration. An incident flux of primary nucleons with energy  $\varepsilon_n$  produces the secondary ion flux with  $\Phi_{sec}(\Lambda)$ . The LET spectrum of secondary particles can be considered to be good metrics when describing not only proton-induced but also neutron-induced

SEUs. GEANT4 can be used as an appropriate tool to simulate the secondary particle LET spectrum  $\Phi_{\text{sec}}(\Lambda)$  at given proton or neutron energy spectra [16–18].

Each particle of nucleon energy corresponds to its own form of the LET spectrum of secondary ions, which can be calculated using GEANT4. Such a procedure is very time-consuming and therefore a simplified and flexible analytical model is highly desirable.

## 2.2. Cross-Section Modeling: Energy Dependence from LET Dependence

For mono-energetic nucleons with a fluence  $\Phi_n$ , we have  $\Phi(\varepsilon_n) = \Phi_n \delta(\varepsilon - \varepsilon_n)$  and  $\Phi_{\text{sec}}(\Lambda) = \alpha(\Lambda|\varepsilon_n)\Phi_n$ . Thus, the conversion function  $\alpha(\Lambda|\varepsilon_n) = \Phi_{\text{sec}}(\Lambda)/\Phi_n$  is simply the LET spectrum of secondary particles normalized to a fluence of primary particles with a given energy. The conversion function can be written in this form:

$$\alpha(\Lambda|\varepsilon_n) = \alpha_n(\varepsilon_n)p(\Lambda|\varepsilon_n), \quad (6)$$

where  $p(\Lambda|\varepsilon_n)$  is normalized to unify the LET spectrum generated by the primary nucleons with energy  $\varepsilon_n$ . The energy dependent efficacy  $\alpha_n(\varepsilon_n)$  can be approximated as follows [19,20]:

$$\alpha_n(\varepsilon_n) \cong \Sigma(\varepsilon_n)N_{at}L_R(\varepsilon_n), \quad (7)$$

where  $N_{at}$  is the atom density in material ( $\sim 5 \times 10^{22} \text{ cm}^{-3}$  in silicon),  $\Sigma(\varepsilon_n)$  is the total cross-section of neutron-nuclear interactions and  $L_R(\varepsilon_n)$  is the mean range of secondary particles. Strictly speaking, the secondary particle generation efficacy  $\alpha_n(\varepsilon_n)$  should also include the average number of the products per nuclear reaction, but this uncertainty can be absorbed by the uncertainty of the secondary particle range which can be considered a fitting parameter. Assuming the maximum value  $\Sigma(\varepsilon_n) \sim 10^{-24} \text{ cm}^2$ , (see, for example, [21]) and  $L_R \geq 1 \mu\text{m}$ , one obtains approximately  $\alpha_n \cong 10^{-5} - 10^{-6}$ . This is an order of magnitude of a ratio of the maximal cross-sections conditioned by nuclear reaction (typically, of order  $10^{-12} - 10^{-14} \text{ cm}^2$  per bit) and heavy ion-induced direct ionization ( $\sim 10^{-7} - 10^{-9} \text{ cm}^2$ ).

Numerical Monte Carlo, analytical and SRIM (see, e.g., [22–24]) simulations have shown that the LET of secondary particles are distributed approximately according to an exponential law up to a certain maximum value  $\Lambda_{\text{max}} \sim 10 - 14 \text{ MeV-cm}^2/\text{mg}$ . Our GEANT4 calculation demonstrates the same picture (see Figure 2).

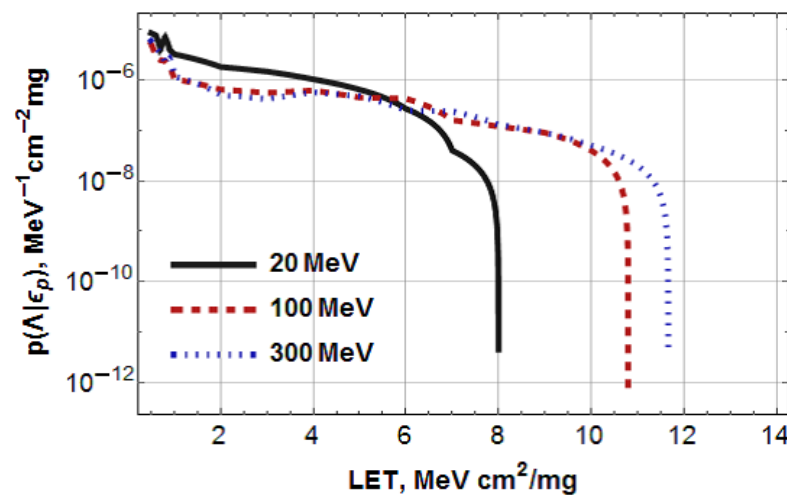


**Figure 2.** GEANT4 simulations of the LET spectra of secondary particles at different proton energies [14].

All Monte Carlo simulations in the article were performed using GEANT4-10.3.0. The LET spectra of secondary particles generally depend on many different factors: nucleon energies, IC layout, geometry, chemical composition of materials, etc. The uncertainty of these factors complicates and reduces the reliability of formally more accurate results. Therefore, we will focus in this study on simple analytical models with physically clear fitting pa-

rameters that can be refined using numerical calculations. The key approximation, which leads to a dramatic simplification of the simulation, is the effective LET approximation, in which the LET spectrum is approximated by a delta function  $p(\Lambda|\varepsilon_n) \cong \delta(\Lambda - \Lambda_{eff}(\varepsilon_n))$ , where  $\Lambda_{eff}(\varepsilon_n)$  is an effective LET which is limited from above by some effective maximum value  $\Lambda_{max} \sim 8\text{--}14 \text{ Mev-cm}^2/\text{mg}$ . The introduction of a fitting parameter  $\Lambda_{eff}(\varepsilon_n)$  allows us to avoid cumbersome numerical integration of ill-defined functions in (5). Indeed, the conversion function takes the form

$$\alpha(\Lambda|\varepsilon_n) \cong \Sigma(\varepsilon_n) N_{at} L_R(\varepsilon_n) \delta(\Lambda - \Lambda_{eff}(\varepsilon_n)), \quad (8)$$

and integration in (5) yields an explicit relation for nuclear-induced SEU cross-section through direct ionization cross-section from secondary heavy ions.

$$\sigma_n(\varepsilon_n) \cong \Sigma(\varepsilon_n) N_{at} L_R(\varepsilon_n) \sigma(\Lambda_{eff}(\varepsilon_n) | Q_C) \quad (9)$$

The next paragraph will be devoted to the parametrization of SEU cross-sections from direct ionization.

### 2.3. Direct Ionization SEU Cross-Section Parametrization

With a decrease in the technological nodes, the threshold energy decreases and the single-event mechanisms begin to play an ever-smaller role. Independence from the mechanism means an increase in the role of statistics, describing the processes without internal correlation. Particularly, the process of ionization and the transfer of energy from radiation to material becomes quantized and is determined more by general statistics. Based on statistical consideration, we found that the SEU cross-section (probability) per bit can be explicitly estimated by the value of the collected charge  $\Delta Q$  during the passage of one ionizing particle [25]:

$$\sigma(\Delta Q) = \frac{a_C}{\exp\left(\frac{Q_C}{\Delta Q}\right) - 1}, \quad (10)$$

where  $a_C$  is the area of the memory cell. Generally, this is in the form of a geometrical or Bose–Einstein distribution. In practice, the only thing that a researcher can experimentally set is the particle’s LET at the input, which is linearly related with  $\Delta Q$ . This makes it possible to rewrite (10) in an approximate form, allowing for direct comparison with the test results:

$$\sigma(\Lambda) = \frac{a_C}{\exp\left(\frac{2\Lambda_C}{\Lambda}\right) - 1} \cong \begin{cases} K_d(\Lambda - \Lambda_C), & \Lambda > \Lambda_C, \\ a_C e^{-\frac{2\Lambda_C}{\Lambda}}, & \Lambda < \Lambda_C, \end{cases} \quad (11)$$

where the slope and threshold of the quasi-linear part of the curve are directly measured experimental parameters connected with the circuit parameters through the relations

$$K_d = \frac{a_C}{2\Lambda_C} \text{ and } \Lambda_C = \frac{\varepsilon_C}{\rho_{Si} t_{eff}}. \quad (12)$$

Here, the silicon mass density is  $\rho_{Si} \cong 2.3 \text{ g/cm}^3$  and  $t_{eff}$  is the effective charge collection length. The “above-threshold case” ( $\Lambda > \Lambda_C$ ) in (11) describes the multiple-cell upset cross-sections ( $\sigma \geq a_C$ ) [26]. The “sub-threshold case”  $\Lambda < \Lambda_C$  corresponds with the Hazucha–Svensson approximation [27]. It should be emphasized that, hereinafter, the critical LET  $\Lambda_C$  will always be understood as the result of an unambiguous interpolation of the linear part of the ion cross-sections  $\sigma(\Lambda)$  (not a Weibull curve parameter) related to  $\varepsilon_C$  and  $Q_C$  by (1) and (11) (see Figure 3).

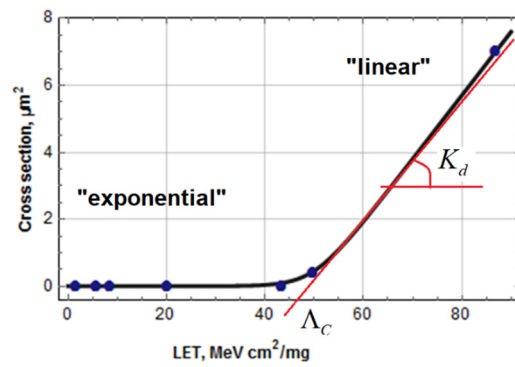


Figure 3. Typical SEU cross-section vs. LET dependence in a linear scale [13].

### 3. Results

#### 3.1. Nucleon-Induced SEU Cross-Sections

The probability of soft errors is proportional to ionization energy deposition and  $\Lambda_{eff}$  in the sensitive region. Experimental data and simulations indicate that zero nucleon energy corresponds to zero  $\Lambda_{eff}$  and, at high  $\epsilon_n$ , the effective LET  $\Lambda_{eff}$  will tend to its maximum value  $\Lambda_{max} \sim 8\text{--}14 \text{ MeV}\cdot\text{cm}^2/\text{mg}$  (see Figure 2). Therefore, it seems reasonable to parameterize  $\Lambda_{eff}(\epsilon_n)$  as a monotonically increasing function of the nucleon energy with saturation at  $\Lambda_{max}$ , such as follows:

$$\Lambda_{eff}(\epsilon_n) \cong \frac{1}{2} \left( \frac{1}{\Lambda_{max}} + \frac{L_R \rho_{Si}}{\epsilon_n} \right)^{-1} \cong \begin{cases} \frac{\epsilon_n}{2\rho_{Si}L_R}, & \epsilon_n < \Lambda_{max}\rho_{Si}L_R, \\ \Lambda_{max}/2, & \epsilon_n > \Lambda_{max}\rho_{Si}L_R, \end{cases} \quad (13)$$

where  $L_R$  (of order of micrometers) is an effective range of secondary ions which can be used as a fitting parameter.

The average LET of secondary ions will increase only up to some threshold neutron energy  $\epsilon_n \leq \epsilon_{nT} = \Lambda_{max}\rho L_R \cong 3.2 (L_R/\mu m) \text{ MeV} \leq 10 \text{ MeV}$  and then saturates at the value  $\Lambda_{max}/2$ . In fact, GEANT4 calculations show that the values  $\Lambda_{max}$  themselves are increasing functions of the energy of primary particles (see, Figure 2) and we will consider  $\Lambda_{max}$  as a fitting parameter. Figure 4 shows rough approximations for the effective LET of secondary particle as functions of neutron energies.

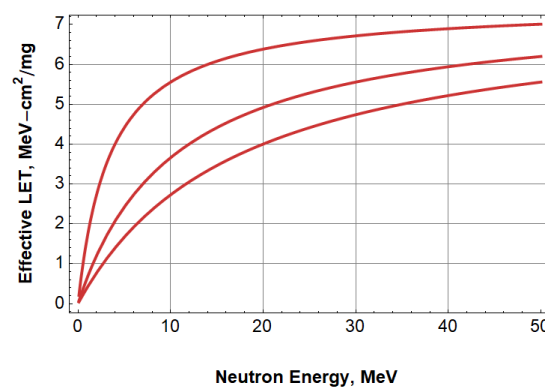


Figure 4. Approximate dependencies of the effective LET on neutron energy  $\Lambda_{eff}(\epsilon_n)$  simulated with (13) at  $\Lambda_{max} = 15 \text{ MeV}\cdot\text{cm}^2/\text{mg}$  for three ion ranges:  $L_R = 1, 3$  and  $5 \mu\text{m}$ .

Following (10) and (12), one can obtain an approximate expression for estimating the energy dependence of the neutron-induced cross-sections:

$$\sigma_n(\epsilon_n) = \frac{\alpha_n(\epsilon_n)a_C}{\exp(2\Lambda_C/\Lambda_{eff}(\epsilon_n)) - 1} \quad (14)$$

where  $\alpha_n$  can be estimated through (11). The neutron-induced nuclear reaction cross-sections at relatively high energies ( $\varepsilon_n \geq 10$  MeV) are approximately constant,  $\Sigma_n^{\max} \sim 1\text{--}2$  bn, whereas the low-energy ( $\varepsilon_n \leq 2$  MeV) cross-sections are usually much smaller, although the behavior of the curve can be very complex [28].

We will roughly approximate the energy dependence of the cross-section for neutron nuclear interactions by using the phenomenological formula

$$\Sigma(\varepsilon_n) \cong \frac{\Sigma_n^{\max}}{1 + \exp\left(-\frac{\varepsilon_n - \varepsilon_{n0}}{\delta\varepsilon_{n0}}\right)}, \quad (15)$$

where  $\varepsilon_{n0}$  and  $\delta\varepsilon_{n0}$  are fitting constants. Figures 5 and 6 show the neutron SEU cross-sections as functions of  $\varepsilon_n$  and circuit parameter  $\Lambda_C$ , analytically simulated with (13)–(15).

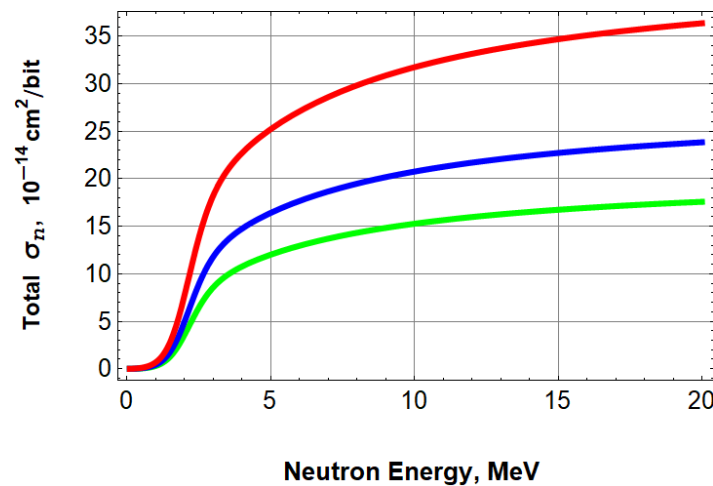


**Figure 5.** Energy dependencies of neutron-induced SEU cross-sections per bit simulated for three values of critical LET (for  $\Lambda_C = 0.2$  (red),  $0.3$  (blue),  $0.4$  (green)  $\text{MeV}\text{-cm}^2/\text{mg}$ ). Parameters:  $a_C = 0.5 \mu\text{m}^2$ ,  $\Lambda_{\max} = 15 \text{ MeV}\text{-cm}^2/\text{mg}$ ,  $\varepsilon_{n0} = 2 \text{ MeV}$ ,  $\delta\varepsilon_{n0} = 0.4 \text{ MeV}$ .

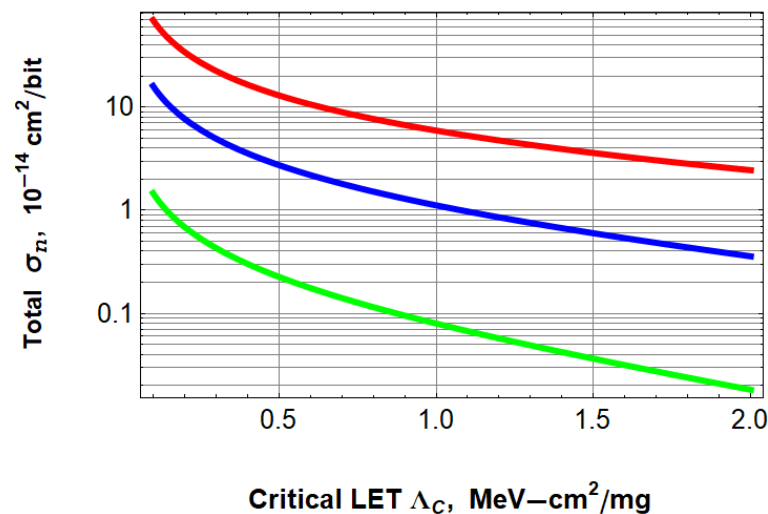


**Figure 6.** Neutron-induced SEU cross-sections per bit simulated as functions of critical LETs for three values of neutron energy (for  $\varepsilon_n = 1$  (green),  $2$  (blue),  $14$  (red)  $\text{MeV}$ ) with the same parameters.

The same Equations (13)–(15) were used to validate the model using the experimental data for proton cross-sections reported in [29] (see Figure 7).

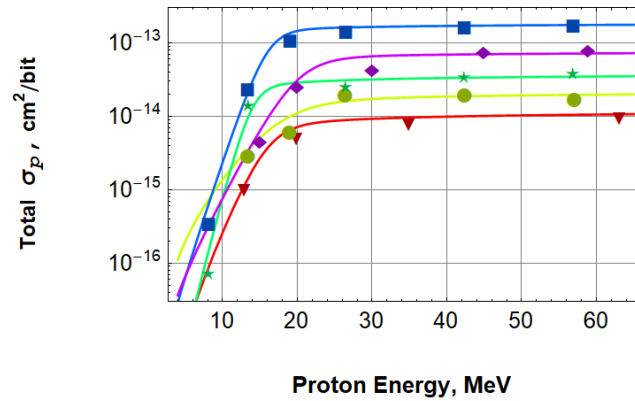


**Figure 7.** Comparison of experimental (points) and simulated (lines) data for proton-induced SEU cross-sections (Lambert et al., 2009 [29]).

The data were simulated with fixed constants  $a_C = 1 \mu\text{m}^2$ ,  $\Lambda_{\text{max}} = 14 \text{ MeV}\cdot\text{cm}^2/\text{mg}$ ,  $L_R = 1 \mu\text{m}$  and  $\Sigma_n^{\text{max}} = 2 \times 10^{-24} \text{ cm}^2$ , while the logarithmic slope and the saturation onset position of the proton cross-section curves in Figure 7 were adjusted by a small change in the parameters  $\delta\varepsilon_{n0}$  (from 1.5 to 3.5 MeV) and  $\varepsilon_{n0}$  (from 14 to 20 MeV). The maximum cross-sections were adjusted by the value of  $\Lambda_C$  (from 1.5 to 7.8  $\text{MeV}\cdot\text{cm}^2/\text{mg}$ ). Any refinement of input parameters (e.g.,  $a_C$  or  $\Sigma_n^{\text{max}}$ ) will reduce the uncertainty of other fitting constants. Thus, unlike the traditional Bendel’s and Weibull’s empirical interpolation [30], the relation (14) is entirely based on transparent physical and circuit approximations and parameters and therefore can be easily modified and recalculated for different IC nodes, chemical compositions of the environment and radiation characteristics.

### 3.2. Proton-Induced SEU Cross-Sections

The total cross-section for proton induction as a function of proton energy can be written as the sum of two cross-sections due to nuclear reactions and direct ionization:

$$\begin{aligned} \sigma_p &\equiv \sigma_{p,\text{nucl}} + \sigma_{p,\text{dir}} = \\ &= \frac{\alpha_p a_C}{e^{2\Lambda_C/\Lambda_{\text{eff}}(\varepsilon_p)} - 1} + \frac{a_C}{e^{2\Lambda_C/\Lambda_p(\varepsilon_p)} - 1} \end{aligned} \quad (16)$$

where  $\alpha_p(\varepsilon_p)$  is the secondary particle generation efficacy which can be simulated with GEANT4 for every specific configuration (see Figure 8 from [14]). The proton efficacy can be parameterized in the same way as for neutrons  $\alpha_p(\varepsilon_p) = N_{at}\Sigma(\varepsilon_p)L_R(\varepsilon_p)$ .

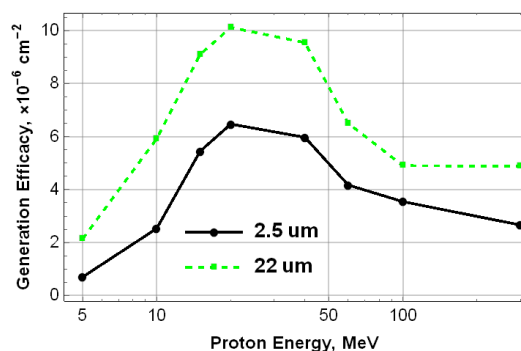


**Figure 8.** The efficacy of secondary particle generation  $\alpha(\varepsilon_p)$  simulated with GEANT4 as a function of proton energies  $\varepsilon_p$  for overlay thicknesses of 2.5  $\mu\text{m}$  (solid line) and 22  $\mu\text{m}$  (dashed line).

Then, that the efficacy decreases with large proton energies can be explained by the energy dependence of the elastic Rutherford scattering  $\Sigma_{\text{Rutherford}}(\varepsilon_p) \propto 1/\varepsilon_p$ , which is the dominant mechanism of nuclear interactions at moderate proton energies. This explains the slight decrease in the SEU cross-section observed at high proton energies. The efficacy

for low-energy protons grows due to an increase in the range of secondary particles  $L_R(\varepsilon_p)$ . The low-energy nuclear reaction cross-sections for protons at low energies (<10 MeV) are typically much smaller than for neutrons due to the presence of the Coulomb barrier. The detailed behavior of nuclear reaction-induced SEU cross-sections for low-energy protons is masked by the direct ionization-induced SEUs. For protons, we will use the same approximation for the effective LET of secondary particles as for neutrons at low energies. The results for the proton SEU cross-sections at high energies usually do not differ much from the case of neutron-induced upsets [31].

The LET  $\Lambda_p(\varepsilon_p)$  of low-energy protons can be simulated using SRIM. A characteristic feature of the proton LET is the presence of a sharp peak at  $\varepsilon_p \sim 50$  keV (see Figure 9).

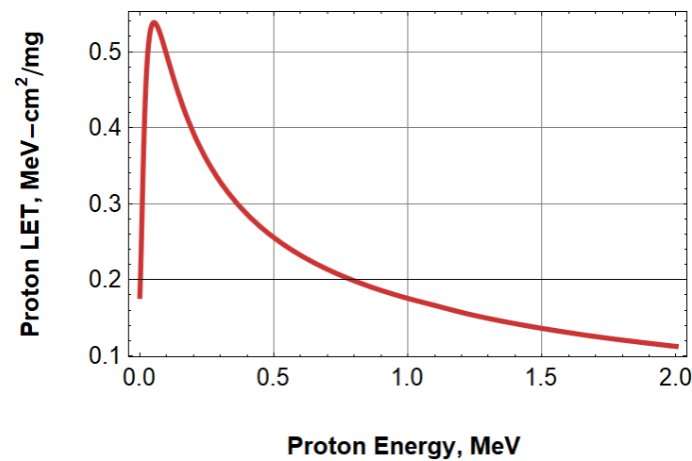


**Figure 9.** SRIM-calculated dependence of LET as a function of proton energy.

For this reason, the calculated dependence of the cross-section on direct ionization must also have a peak approximately at this energy. The SEU cross-sections are monotonically decreasing functions of the parameter  $\Lambda_C$  (see Figure 10).

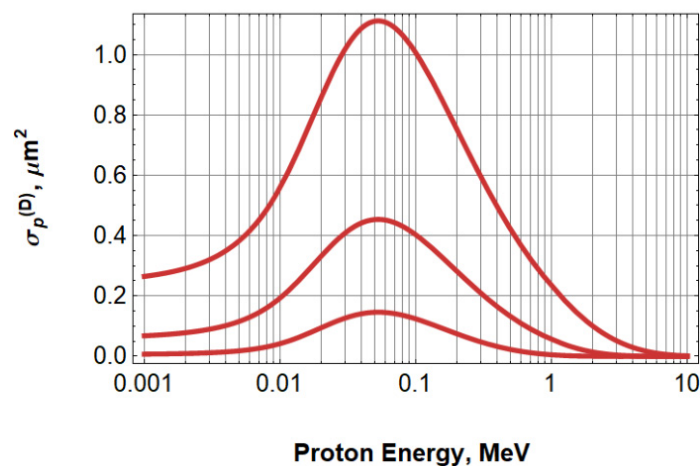


**Figure 10.** Non-monotonic view of direct ionization SEU cross-sections for low-energy protons simulated with Equation (16) for different  $\Lambda_C$ ;  $\Lambda_p(\varepsilon_p)$  was simulated using SRIM as in Figure 9.

The specific form of the dependence of the total cross-section on the proton energy, including direct and indirect ionization, is determined by the circuit parameter  $\Lambda_C$ , as shown in the illustrative simulation in Figure 11.

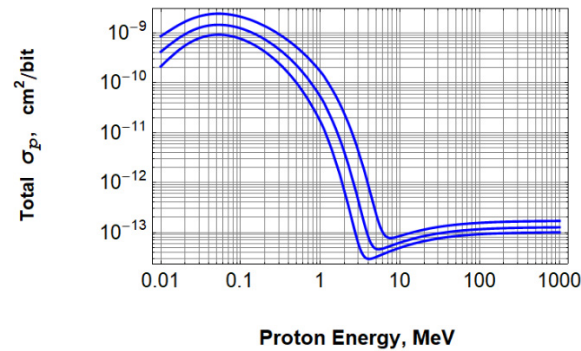


**Figure 11.** Typical proton-induced SEU cross-sections as a function of energy, simulated with Equation (16) for critical LETs:  $\Lambda_C = 0.3, 0.4, 0.5$  MeV·cm<sup>2</sup>/mg (top down).

In practice, there is a problem associated with the fact that the low-energy proton energy spectra are formed by the specifics of local shielding, which makes it difficult to simulate due to the difference in the energies of external protons and directly ionizing internal protons. As the proton energy increases to about 10 MeV, the proton LET decreases and the total SEU cross-section drops exponentially (see Equation (16)) to the level of nuclear-induced effects. The results of the model validation are shown in Figure 12 where the comparison of calculation results and recent experimental data (adopted from Figure 1 in [32]) is presented.

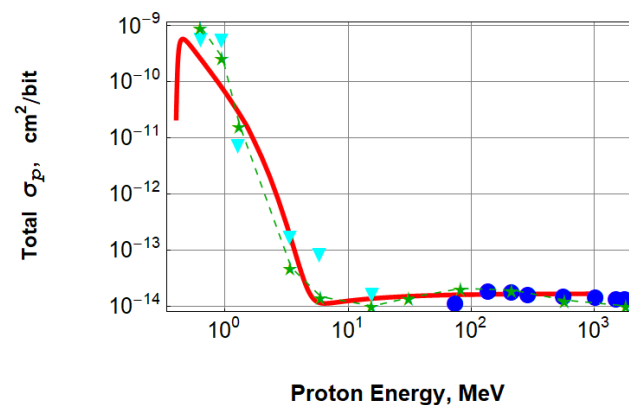


**Figure 12.** A comparison of experimental total proton cross-sections vs. energy (different points) and simulation with (16) (red solid line).

Simulated proton-induced SEU cross-sections are in reasonable agreement in exponentially wide ranges of cross-sections at low-, intermediate- and high-energy protons at 14 MeV neutrons. Fitting parameters were  $a_C = 0.1 \mu\text{m}^2$ ,  $\Lambda_{\text{max}} = 6$  MeV·cm<sup>2</sup>/mg,  $\Lambda_C = 0.4$  MeV·cm<sup>2</sup>/mg and  $L_R = 1 \mu\text{m}$ ,  $\Sigma_n^{\text{max}} = 1 \times 10^{-24}$  cm<sup>2</sup>.

#### 4. Discussion

In this study, we proposed a general computational scheme for estimating the cross-sections of SEU induced by direct ionization and nuclear interactions (Equations (2)–(5), (10) and (11)) and its simplified analytical implementation (Equations (8), (9), (13) and (15)). The weakest point of the proposed simplified computational scheme is the method for roughly estimating the effective LET (Equation (13)). A more rigorous approach involves averaging over the exponential LET spectrum of secondary particles (see Equations (5) and (6)), which strictly speaking can only be calculated using the GEANT4 simulation. Any advanced numerical simulation makes sense in the presence of very detailed input data, which is not available in practice. Therefore, such calculations require cumbersome additional calibration, which is not much different from the simple fitting of one parameter within a simplified analytical model.

The main conceptual differences of the proposed approach compared to existing ones are as follows:

- Our proposed method consistently derives the nuclear-induced SEU cross-section as a result of direct ionization by secondary particles. This allows the two failure mechanisms to be described in a unified manner within the same mathematical formalism.
- The generalized relation (10) is used instead of the Hazucha–Svensson formula, which is a special case of (10) for large values of the critical charge.
- This allows us to describe multiple-cell upsets and the SEUs at very low-energy deposits during direct ionization of low-energy protons.
- Unlike our approach, the traditional burst generation rate (BGR) method proposed by Ziegler and Lanford [33] is entirely based on the computation of nuclear effects and does not include critically important technological parameters such as a memory cell area  $a_C$ . The BGR method is valid only when the sensitive volume is so large that energy deposition can be taken locally.

A new physics-based compact model, which makes it possible to simulate in a unified way the neutrons and protons of cosmic ray-induced SEU cross-sections, including the effects from nuclear reaction products and from direct ionization by low-energy protons, has been proposed and validated. To summarize, we list the main advantages of the described unified approach in terms of simplicity and realism (analytical equations with physical and circuit parameters):

- Universality (both for neutrons and protons);
- Generality (the same approach to direct ionization and nuclear reaction-induced effects);
- Compatibility with circuit simulations (critical charge/energy, cell area, etc.);
- Compatibility with radiation simulations (GEANT4, SRIM, etc.);
- Flexibility (can be refined by numerical simulations and adapted to suit different purposes).

**Author Contributions:** Conceptualization, G.I.Z.; data curation, V.V.E.; formal analysis, R.G.U.; funding acquisition, N.N.S.; investigation, R.G.U.; methodology, G.I.Z.; software, A.M.G. and A.A.S.; supervision, N.N.S. and A.S.R.; visualization, D.A.K.; writing—original draft, G.I.Z. and R.G.U.; writing—review and editing, N.N.S. and A.S.R. All authors have read and agreed to the published version of the manuscript.

**Funding:** This work was carried out within the framework of the state task of the Ministry of Science and Higher Education of the Russian Federation (subject No. FSWU-2022-0022 “Low-temperature ceramic technologies (LTCC) in microelectronics”).

**Institutional Review Board Statement:** Not applicable.

**Informed Consent Statement:** Not applicable.

**Data Availability Statement:** The data presented in this study are available in this article.

**Conflicts of Interest:** The authors declare no conflicts of interest. The funders had no role in the design of the study; in the collection, analyses, or interpretation of data; in the writing of the manuscript; or in the decision to publish the results.

## References

1. Petersen, E.L.; Koga, R.; Shoga, M.A.; Pickel, J.C.; Price, W.E. The Single Event Revolution. *IEEE Trans. Nucl. Sci.* **2013**, *60*, 1824–1835. [[CrossRef](#)]
2. Single-Event Analysis and Prediction. Available online: <https://iee-npss.org/wp-content/uploads/2021/11/1997-NSREC.pdf> (accessed on 26 December 2023).
3. Heidel, D.F.; Marshall, P.W.; LaBel, K.A.; Schwank, J.R.; Rodbell, K.P.; Hakey, M.C.; Berg, M.D.; Dodd, P.E.; Friendlich, M.R.; Phan, A.D.; et al. Low Energy Proton Single-Event-Upset Test Results on 65 nm SOI SRAM. *IEEE Trans. Nucl. Sci.* **2008**, *55*, 3394–3400. [[CrossRef](#)]
4. Rodbell, K.P.; Heidel, D.F.; Tang, H.H.K.; Gordon, M.S.; Oldiges, P.; Murray, C.E. Low-Energy Proton-Induced Single-Event-Upsets in 65 nm Node, Silicon-on-Insulator, Latches and Memory Cells. *IEEE Trans. Nucl. Sci.* **2007**, *54*, 2474–2479. [[CrossRef](#)]

5. Lüdeke, S.; Cardenás, G.D.; Hajdas, W.; Jaatinen, J.; Kettunen, H.; Poivey, C.; Rossi, M.; Tanios, B.; Vogiatzi, S.M.; Javanainen, A. Proton Direct Ionization in Sub-Micron Technologies: Test Methodologies and Modelling. *IEEE Trans. Nucl. Sci.* **2023**, *70*, 667–677. [[CrossRef](#)]
6. Chen, W.; Guo, X.; Wang, C.; Zhang, F.; Qi, C.; Wang, X.; Jin, X.; Wei, Y.; Yang, S.; Song, Z. Single-Event Upsets in SRAMs with Scaling Technology Nodes Induced by Terrestrial, Nuclear Reactor, and Monoenergetic Neutrons. *IEEE Trans. Nucl. Sci.* **2019**, *66*, 856–865. [[CrossRef](#)]
7. Fuketa, H.; Hashimoto, M.; Mitsuyama, Y.; Onoye, T. Neutron-Induced Soft Errors and Multiple Cell Upsets in 65-nm 10T Subthreshold SRAM. *IEEE Trans. Nucl. Sci.* **2011**, *58*, 2097–2102. [[CrossRef](#)]
8. He, Y.; Lei, Z.; Zhang, Z.; Peng, C.; Li, J.; Zhang, E.; Yang, Y. Analysis of Atmospheric Neutron Radiation Effects in Automotive Electronics Systems. In Proceedings of the 2020 IEEE International Symposium on the Physical and Failure Analysis of Integrated Circuits (IPFA), Singapore, 20–23 July 2020; pp. 1–4. [[CrossRef](#)]
9. Gordon, M.S.; Goldhagen, P.; Rodbell, K.; Zabel, T.; Tang, H.; Clem, J.; Bailey, P. Measurement of the flux and energy spectrum of cosmic-ray induced neutrons on the ground. *IEEE Trans. Nucl. Sci.* **2004**, *51*, 3427–3434. [[CrossRef](#)]
10. Reed, R.A.; Weller, R.A.; Mendenhall, M.H.; Fleetwood, D.M.; Warren, K.M.; Sierawski, B.D.; King, M.P.; Schrimpf, R.D.; Auden, E.C. Physical Processes and Applications of the Monte Carlo Radiative Energy Deposition (MRED) Code. *IEEE Trans. Nucl. Sci.* **2015**, *62*, 1441–1461. [[CrossRef](#)]
11. Sierawski, B.D.; Pellish, J.A.; Reed, R.A.; Schrimpf, R.D.; Warren, K.M.; Weller, R.A.; Mendenhall, M.H.; Black, J.D.; Tipton, A.D.; Xapsos, M.A.; et al. Impact of Low-Energy Proton Induced Upsets on Test Methods and Rate Predictions. *IEEE Trans. Nucl. Sci.* **2009**, *56*, 3085–3092. [[CrossRef](#)]
12. Mo, L.-H.; Ye, B.; Liu, J.; Luo, J.; Sun, Y.-M.; Cai, C.; Li, D.-Q.; Zhao, P.-X.; He, Z. Neutron-induced single event upset simulation in Geant4 for three-dimensional die-stacked SRAM. *Chin. Phys. B* **2020**, *30*, 036103. [[CrossRef](#)]
13. Dodd, P.E.; Shaneyfelt, A.; Horn, K.; Walsh, D.; Hash, G.; Hill, T.; Draper, B.; Schwank, J.; Sexton, F.; Winokur, P. SEU-sensitive volumes in bulk and SOI SRAMs from first-principles calculations and experiments. *IEEE Trans. Nucl. Sci.* **2001**, *48*, 1893–1903. [[CrossRef](#)]
14. Zebrev, G.I.; Galimov, A.M. Compact Modeling and Simulation of Heavy Ion-Induced Soft Error Rate in Space Environment: Principles and Validation. *IEEE Trans. Nucl. Sci.* **2017**, *64*, 2129–2135. [[CrossRef](#)]
15. Galimov, A.M.; Galimova, R.M.; Zebrev, G.I. GEANT4 simulation of nuclear interaction induced soft errors in digital nanoscale electronics: Interrelation between proton and heavy ion impacts. *Nucl. Instrum. Methods Phys. Res. Sect. A* **2019**, *913*, 65–71. [[CrossRef](#)]
16. Inguibert, C.; Duzellier, S. SEU rate calculation with GEANT4 (comparison with CREME 86). *IEEE Trans. Nucl. Sci.* **2004**, *51*, 2805–2810. [[CrossRef](#)]
17. Outil de Modélisation de l’Environnement Radiatif Externe OMERE. Available online: <http://www.trad.fr/OMERE-Software.html> (accessed on 13 February 2024).
18. O’Neill, P.M.; Badhwar, G.D.; Culpepper, W.X. Internuclear cascade-evaporation model for LET spectra of 200 MeV protons used for parts testing. *IEEE Trans. Nucl. Sci.* **1998**, *45*, 2467–2474. [[CrossRef](#)] [[PubMed](#)]
19. Zebrev, G.I. Modeling neutron ionization effects on high-density CMOS circuit elements. *Russ. Microelectron.* **2006**, *35*, 185–196. [[CrossRef](#)]
20. Zebrev, G.I.; Ishutin, I.O.; Useinov, R.G.; Anashin, V.S. Methodology of Soft Error Rate Computation in Modern Microelectronics. *IEEE Trans. Nucl. Sci.* **2010**, *57*, 3725–3733. [[CrossRef](#)]
21. Inguibert, C.; Duzellier, S.; Nuns, T.; Bezerra, F. Using Subthreshold Heavy Ion Upset Cross Section to Calculate Proton Sensitivity. *IEEE Trans. Nucl. Sci.* **2007**, *54*, 2394–2399. [[CrossRef](#)]
22. Hiemstra, D.M.; Blackmore, E.W. LET spectra of proton energy levels from 50 to 500 MeV and their effectiveness for single event effects characterization of microelectronics. *IEEE Trans. Nucl. Sci.* **2003**, *50*, 2245–2250. [[CrossRef](#)]
23. Chen, W. Irradiation Testing and Simulation of Neutron-induced Single Event Effects. In Proceedings of the 26th International Seminar on Interaction of Neutrons with Nuclei, Xi’an, China, 28 May 2018.
24. Haran, A.; Barak, J.; Weissman, L.; David, D.; Keren, E. 14 MeV Neutrons SEU Cross Sections in Deep Submicron Devices Calculated Using Heavy Ion SEU Cross Sections. *IEEE Trans. Nucl. Sci.* **2011**, *58*, 848–854. [[CrossRef](#)]
25. Zebrev, G.I. Single Event Concepts and Characterization. In Proceedings of the 4th International Conference on Radiation Effects of Electronic Devices, Xi’an, China, 26–29 May 2021.
26. Zebrev, G.; Gorbunov, M.; Useinov, R.; Emelianov, V.; Ozerov, A.; Anashin, V.; Kozyukov, A.; Zemtsov, K. Statistics and methodology of multiple cell upset characterization under heavy ion irradiation. *Nucl. Instrum. Methods Phys. Res. Sect. A* **2015**, *775*, 41–45. [[CrossRef](#)]
27. Hazucha, P.; Svensson, C. Impact of CMOS technology scaling on the atmospheric neutron soft error rate. *IEEE Trans. Nucl. Sci.* **2000**, *47*, 2586–2594. [[CrossRef](#)]
28. Cecchetto, M. Experimental and Simulation Study of Neutron-Induced Single Event Effects in Accelerator Environment and Implications on Qualification Approach. Ph.D. Thesis, Montpellier University, Montpellier, France, 2021. Available online: <https://tel.archives-ouvertes.fr/tel-03391539> (accessed on 13 February 2024).

29. Lambert, D.; Desnoyers, F.; Thouvenot, D. Investigation of neutron and proton SEU cross-sections on SRAMs between a few MeV and 50 MeV. In Proceedings of the 2009 European Conference on Radiation and Its Effects on Components and Systems, Brugge, Belgium, 14–17 September 2009; pp. 148–154. [[CrossRef](#)]
30. Bendel, W.L.; Petersen, E.L. Proton Upsets in Orbit. *IEEE Trans. Nucl. Sci.* **1983**, *30*, 4481–4485. [[CrossRef](#)]
31. Granlund, T.; Olsson, N. A Comparative Study Between Proton and Neutron Induced SEUs in SRAMs. *IEEE Trans. Nucl. Sci.* **2006**, *53*, 1871–1875. [[CrossRef](#)]
32. Coronetti, A.; Alía, R.G.; Lucsanyi, D.; Wang, J.; Saigné, F.; Javanainen, A.; Leroux, P.; Prinzie, J. Proton direct ionization upsets at tens of MeV. *IEEE Trans. Nucl. Sci.* **2022**, *70*, 314–321. [[CrossRef](#)]
33. Ziegler, J.F.; Lanford, W.A. The effect of cosmic rays on computer memories. *Science* **1979**, *206*, 776–788. [[CrossRef](#)] [[PubMed](#)]

**Disclaimer/Publisher’s Note:** The statements, opinions and data contained in all publications are solely those of the individual author(s) and contributor(s) and not of MDPI and/or the editor(s). MDPI and/or the editor(s) disclaim responsibility for any injury to people or property resulting from any ideas, methods, instructions or products referred to in the content.